

An Experimental Introduction to Colloidal Nanocrystals through InP and InP/ZnS Quantum Dots

Mahsa Parvizia, Julia Bechter, Jan Huber, Noura Chettata, and Jonathan De Roo*



Cite This: *J. Chem. Educ.* 2023, 100, 1613–1620



Read Online

ACCESS |



Metrics & More



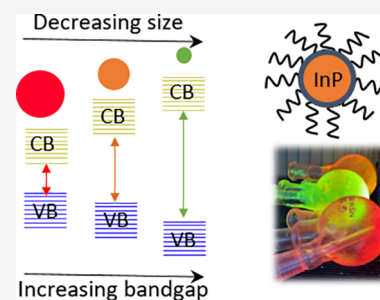
Article Recommendations



Supporting Information

ABSTRACT: Quantum dots are colloidal semiconductor nanocrystals that display size-dependent electronic and optical properties. These materials are a visual demonstration of a quantum-mechanical effect. Here we present a laboratory exercise for undergraduate/Bachelor students as an introduction to colloidal nanocrystals and quantum dots. The students synthesize three sizes of indium phosphide (InP) nanocrystals and perform one core/shell synthesis of indium phosphide cores shelled with zinc sulfide (InP/ZnS). The obtained quantum dots are characterized by quantitative UV–vis, photoluminescence, and ^1H NMR spectroscopy. Students are acquainted with several concepts: nanocrystal synthesis, colloids, Beer–Lambert law, quantum confinement, photoluminescence, and surface chemistry. For each concept, background information is provided, rendering this report a comprehensive introduction for students and teachers. Indium phosphide is a safer material to handle in the undergraduate lab compared to cadmium selenide (CdSe), cesium lead bromide (CsPbBr₃), or lead sulfide (PbS) nanocrystals.

KEYWORDS: *Hands-On Learning/Manipulatives, Laboratory Instruction, Inorganic Chemistry, Nanotechnology, Upper-Division Undergraduate, Materials Science*



INTRODUCTION

Nanocrystals present size-dependent properties that cannot be obtained in the bulk material.^{1–4} In nanocrystal synthesis, we aim to control the size and shape of the particles in order to obtain colloids with a narrow size distribution.^{5–9} Quantum dots (QDs) are *semiconductor* nanocrystals, typically with a diameter of 2–10 nm.¹⁰ QDs display size-dependent electronic and optical properties due to *quantum confinement*.^{10–12} This effect is similar to the classical “particle in a box” problem, and therefore, QDs are a unique visual manifestation of a quantum-mechanical effect.

QDs are often made via a colloidal synthesis.^{5,7,13,14} This bottom-up approach assembles atoms into nanocrystals that contain thousands of atoms in an ordered lattice. The complex process is a controlled precipitation and a crystallization reaction. There are three essential components: precursors, solvent, and ligands.^{15,16} Molecular precursors convert into the nanocrystal core. Chemically stable solvents with a high boiling point are required,¹⁵ since the inorganic core typically crystallizes between 200 and 350 °C. Ligands are essential to stabilize the QDs against aggregation and regulate QD growth.^{5,6} The most commonly used ligands are surfactants: amphiphilic molecules with a polar head (binding group) and a long aliphatic tail. The latter provides the QD with solubility in nonpolar solvents.^{5,17–19} For more information on colloidal nanocrystal synthesis, we refer to reviews.^{15,20–22}

Part of the synthetic effort lies in isolating and purifying the synthesized QD products.¹⁵ Byproducts, side products, excess

ligands, and the (high-boiling) solvent are to be removed. The precipitation–redispersion method relies on polarity differences. QDs with hydrophobic ligands are soluble in nonpolar solvents (e.g., toluene) and precipitate upon the addition of polar solvents (e.g., methanol). After centrifugation, the supernatant (including impurities) is decanted, and the compacted precipitate is redispersed. Multiple cycles of precipitation–redispersion are necessary to remove all impurities. Alternatively, size exclusion chromatography (SEC) separates QDs from small molecules based on size.^{23,24} It uses a porous gel (cross-linked polymer) as the stationary phase. The retention time is size-dependent since small molecules are trapped in the small pores while bigger objects stay in the mobile phase. For more information, we refer to an excellent review on nanocrystal purification.²⁵

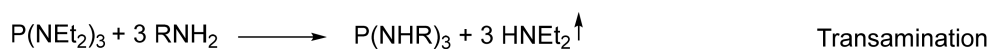
The QD field is a multidisciplinary one, connecting with all traditional disciplines of chemistry as well as materials science, physics, engineering, and biology. We have introduced QD experiments in our inorganic chemistry laboratory course, but they could equally well be included in physical chemistry practical courses. Unfortunately, most educational materials on

Received: December 10, 2022

Revised: March 10, 2023

Published: March 28, 2023



Scheme 1. Relevant Chemical Equations for the Synthesis of InP from Indium Halide and Tris(diethylamino)phosphine in the Presence of Oleylamine (RNH₂)


QDs are based on toxic elements, e.g., CdSe, CsPbBr₃, and PbS.^{26–30} ZnS and ZnSe have a high band gap and do not cover the visible spectrum.^{31–34} Recently, an educational experiment introduced Zn_{2x}Cu_{1-x}In_{1-x}S₂ QDs³⁵ with tunable emission over the visible range. However, the QDs did not have a well-defined first excitonic peak. Industrially, the leading cadmium-free and lead-free technology is based on indium phosphide (InP),^{36,37} but there are no undergraduate experiments available.

Here we present a safer laboratory experiment that familiarizes the student with important concepts in QD synthesis, surface chemistry, and optical properties while also teaching basic chemical laboratory techniques. The students first learn to synthesize three different sizes of InP QDs and characterize their optical properties. Second, the students synthesize an InP/ZnS core/shell structure. We have successfully implemented this experiment in an inorganic chemistry laboratory course for 20 undergraduate students at the University of Basel. They had one full day and two half days to perform the syntheses and to fully characterize the products using UV–vis, photoluminescence, and NMR spectroscopy. The students discussed their results in an article-style report. The learning objectives of these experiments are as follows:

- Ability to work in a group
- Mastering air-free and Schlenk techniques, including air-free transfer of liquids
- Handling a heating mantle (optional)
- Mastering the precipitation–redispersion purification technique
- Mastering size exclusion chromatography as a purification technique (optional)
- Acquisition and interpretation of UV–vis and photoluminescence spectra; interpretation of quantum confinement; use of the Beer–Lambert law to calculate QD concentration; use of a sizing curve to calculate the QD size.
- Acquisition and interpretation of ¹H NMR spectra for ligand-capped particles and stripped particles; identification of the ligand via reference spectra

RESULTS AND DISCUSSION

Chemistry of InP Synthesis

Indium halides react at 180 °C with tris(diethylamino)phosphine in the presence of oleylamine to form InP QDs. Different sizes of InP QDs are made by starting from different indium halides.³⁸ The role of oleylamine is threefold: it is the solvent, it is the only ligand present, and it is also involved in the reaction mechanism (see Scheme 1). In the first step, transamination occurs between the original aminophosphine

and the primary amine (oleylamine) in the solution. In the second step, disproportionation of the tris(oleylamino)phosphine takes place.^{39,40} Indium has the same (+III) oxidation state in both the precursor and the final InP product. However, phosphorus has a (+III) oxidation state in the (RNH)₃P compound and is present in the (–III) oxidation state in the final product. Tris(oleylamino)phosphine (3 equiv) reduces tris(oleylamino)phosphine (1 equiv) to P(–III) and is oxidized to P(+V) in the P(NHR)₄Cl phosphonium salt. The entire balanced equation is shown in Scheme 1. For the formation of 1 mol of InP, 12 mol of primary amine and 4 mol of aminophosphine are required.

Zinc chloride is added to the reaction mixture to reduce the size dispersion of the InP cores, although its role in the mechanism is currently poorly understood. In the synthesis of InP/ZnS core/shell QDs, zinc chloride is supposed to be an active reagent.

Introduction to Quantum Confinement

After injection of the aminophosphine precursor, the initially colorless solution gradually turns dark red within 20 min. Students take aliquots every 5 min after injection, thus observing QD growth visually and quantitatively using UV–vis spectroscopy (Figure 1). A progressive shift of the first excitonic peak toward longer wavelengths (i.e., a red shift) is observed. All data shown in this article were obtained by students. To explain the observations, we turn to quantum mechanics.

The particle in a box (also called the infinite potential well) is usually the first quantum-mechanical problem that students tackle. When solving the corresponding Schrödinger equation, one obtains the wave functions and energies for the eigenstates. For a simple one-dimensional box, the energy is given by eq 1:

$$E_n = \frac{\hbar^2 n^2 \pi^2}{2ma^2} \quad (1)$$

The energy is proportional to the square of the quantum number (*n*) and *inversely* proportional to the mass of the particle (*m*) and the potential well width (*a*). A smaller box leads to a higher energy of the particle, even for the ground state (*n* = 1). In other words, more energy is required to confine a particle in a smaller space. This phenomenon is called quantum confinement. The effect is negligible on the macro level but significant once the box is only a few nanometers large.

For a semiconducting material like InP, there is a filled valence band and an empty conduction band with a relatively small gap between the bands (i.e., the band gap). An incident photon that has an energy lower than the band gap will not be absorbed (absorbance = 0 in UV–vis). If the photon energy

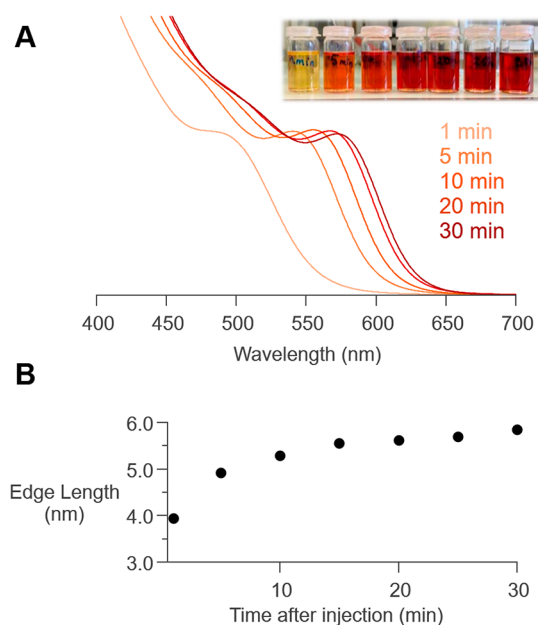


Figure 1. (A) Normalized absorption spectra of the aliquots taken during the large core synthesis of InP (using InCl_3). The maximum absorption peak shifts to a longer wavelength as the QDs grow over time. A picture of the diluted aliquots under visible-light illumination is shown as an inset. The reaction time increases from left to right. (B) The calculated sizes for the different aliquots are plotted versus the time at which the aliquots are taken. The timing starts right after the $(\text{Et}_2\text{N})_3\text{P}$ injection.

matches the band gap energy, the photon is absorbed, promoting an electron to the conduction band and leaving behind a hole. This electron–hole pair is called an exciton. The absorption of the photon results in an absorption feature in the UV–vis spectrum, called the first excitonic peak. If the photon has even higher energy (shorter wavelength), more transitions to higher energy levels are available, and stronger UV–vis absorption is observed (see Figure 1).

Unlike a bulk semiconductor, the band gap of the InP nanocrystals is not a fixed value. Given that the electron in the conduction band and the hole in the valence band are confined to the size of the nanocrystals, there is an additional price to pay: the confinement energy. The confinement energy is higher for smaller nanocrystals. Hence, one observes a shift of the first excitonic peak to longer wavelength (lower energy) when the particles are growing.

Calculation of QD Sizes from UV–Vis Data

The average QD size can be determined for every aliquot by applying the following sizing formula to the UV–vis data (eq 2):^{41,42}

$$L_{\text{NC}} = \left(\frac{C}{E_{\text{NC}} - E_{\text{bulk}}} \right)^{1/\alpha} \quad (2)$$

where L_{NC} is the average QD edge length (in nm), E_{NC} is the energy of the band edge transition at the maximum absorbance of the obtained particles (in eV), E_{bulk} is the bulk band gap of InP (1.35 eV), and C and α are empirically derived fitting parameters (4.25 and 0.96, respectively). The sizing curve is different for tetrahedral and spherical particles. In the original synthesis paper,³⁸ the authors assumed a spherical shape, but later it was proven that the InP QDs synthesized from indium

halides and oleylamine have a tetrahedral shape.⁴² Therefore, the students will calculate a different edge length than the originally reported diameter.

After 1 min of reaction, the particles have an average size of 3.8 nm when starting from InCl_3 (see Figure 1B). The size slowly increases to 5.8 nm. The growth mainly occurs during the first 10 min. The students obtained on average (averaged over all student teams) an edge length of 6 nm for the large particles, 5 nm for the medium-sized particles, and 4 nm for the small particles.

Structural Analysis

Powder X-ray diffraction (XRD) is a method to determine or confirm the atomic arrangement of a material, i.e., the crystal phase. Incident X-rays scatter from a lattice of atoms. Constructive interference of the scattered waves happens when Bragg's law is satisfied (eq 3):

$$n\lambda = 2d \sin \theta \quad (3)$$

where λ the wavelength of the X-ray, d is the distance between lattice planes, and θ is the scattering angle. XRD characterization might not always be available for an undergraduate lab. Therefore, we recommend measuring it once and only providing the diffractogram to the students (see Figure 2).

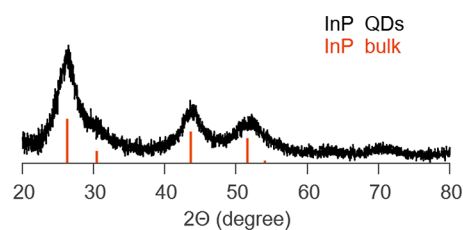


Figure 2. Diffractogram of the synthesized large InP QD cores compared with the reference of bulk InP. The peaks are broader compared to the bulk due to the small size of the QDs.

The Bragg peaks are broadened due to the small crystal size, but the agreement with the reference diffractogram of zinc blende InP is clear. The crystallite size, D , can be calculated using the Scherrer equation:

$$D = \frac{0.9\lambda}{\beta \cos \theta} \quad (4)$$

where β is the full width at half-maximum of the Bragg peak. More information about XRD is found in the references.^{43,44}

Photoluminescence

All of the final solutions were visually red in normal light and emitted green, orange, and red colors under UV illumination for the small, medium, and large QDs, respectively (Figure 3). The absorption of UV light creates an electron–hole pair (an exciton). This electron–hole pair can recombine in a couple of nanoseconds to emit a photon (i.e., photoluminescence). The photon energy is typically that of the band gap since electrons and holes first relax to the lowest-energy state of the conduction and valence band respectively, before recombining. The shoulder/second feature at higher wavelength is typically attributed to emission from trap states (defects on the surface).⁴⁵

The efficiency of radiative recombination is expressed as the photoluminescence quantum yield (PLQY):

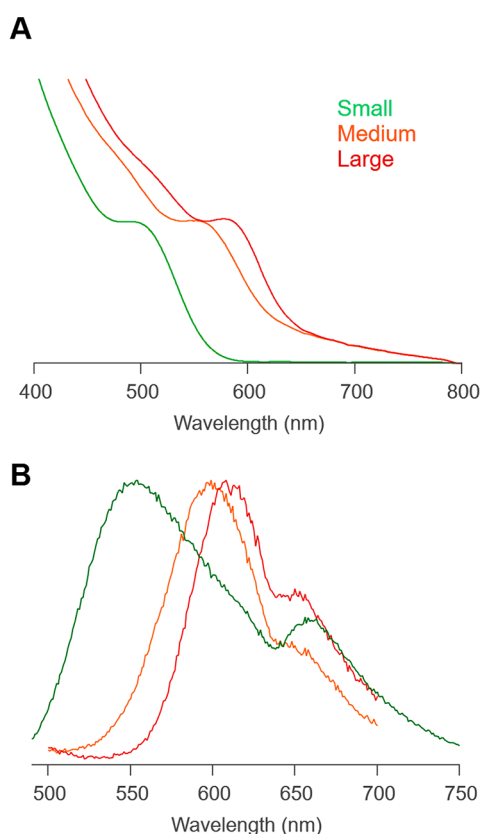


Figure 3. Normalized absorption and photoluminescence spectra of the three synthesized cores.

$$\text{PLQY} = \frac{\text{emitted photons}}{\text{absorbed photons}} \quad (5)$$

The photoluminescence of the InP cores is rather weak, and we will come back to this point in [Core/Shell Synthesis and Photoluminescence](#).

Calculation of QD Concentration by UV–Vis Spectroscopy

In chemistry, yield is an important metric. The concentration and thus the yield of the obtained InP QDs is determined by UV–vis spectroscopy. The intrinsic absorption coefficient of a QD material, μ_i , is size-independent at sufficiently short wavelengths. The absorbance scales with the volume fraction, f , of QD material in solution according to⁴⁶

$$A = \frac{\mu_i f L}{\ln 10} \quad (6)$$

where L is the path length of the cuvette (in m). To make the bridge to the Beer–Lambert law, it is useful to calculate the molar extinction coefficient, ϵ , from this intrinsic absorption coefficient (eq 7):

$$\epsilon = \frac{N_A V_{\text{QD}}}{\ln 10} \mu_{i,413} \quad (7)$$

where N_A is the Avogadro number, V_{QD} is the average volume of the QDs, and $\mu_{i,413}$ ($8.5 \times 10^6 \text{ m}^{-1}$) is the intrinsic absorption coefficient of InP at 413 nm.³⁸ The extinction coefficient is wavelength-dependent, so the absorbance at 413 nm should be used. The molar extinction coefficient is size-dependent, since it scales with the volume of a single QD. Indeed, the same amount of InP could be distributed over

many small particles or over a few large particles. This would not change the absorption, but it would translate into a different particle concentration. The students use the obtained molar extinction coefficient with the Beer–Lambert law to calculate the concentration of QDs in the cuvette.

Once the concentration in the cuvette has been obtained, students can calculate the concentration in their stock solution by taking into account the dilution necessary for the UV–vis measurement. From there, one can calculate the yield.

A more straightforward determination of the yield goes via the volume fraction. The volume fraction f of InP in the cuvette can be determined using the measured absorbance A and the intrinsic absorption coefficient of InP at 413 nm, $\mu_{i,413}$, according to eq 8:

$$f = \frac{A \ln 10}{\mu_{i,413} L} \quad (8)$$

Taking into account the dilution, the volume fraction in the stock solution, f_{stock} , is calculated. Using the total volume of stock solution (V_{stock}) and the molar volume of InP ($V_{\text{M,InP}} = 30.3 \text{ cm}^3 \text{ mol}^{-1}$), one calculates the molar amount of InP (n_{InP}) according to eq 9:

$$n_{\text{InP}} = \frac{f_{\text{stock}} V_{\text{stock}}}{V_{\text{M,InP}}} \quad (9)$$

Finally, the reaction yield is determined. Students obtained yields between 27% and 50% after purification.

Core/Shell QD Synthesis and Photoluminescence

The surface of a QD is highly exposed to its surroundings (solvents, ligands, etc.), which has a strong effect on the optical properties.^{47–49} In addition, surface atoms have a different coordination compared to the bulk atoms since the lattice is abruptly terminated. This can lead to localized energy states that are not part of the conduction or valence band. These states are called surface traps since they provide pathways for nonradiative exciton recombination, which reduce the PLQY. One of the methods to remove trap states is to grow a shell of a wider-band-gap material around the QDs. The interface between two layers of different semiconductors is called a heterojunction.⁵⁰ For our discussion here, we focus on the type-I heterojunction, where the conduction-band minimum of the shell is higher than that of the core and the valence-band maximum of the shell is lower than that of the core (Figure 4). Such an architecture creates a potential well that confines the electrons and holes to the core, avoiding interaction with surface trap states and surrounding media.^{51–54} The InP/ZnS core/shell QD is an example of such a type-I heterostructure.

Experimentally, the previously described synthesized cores show very low luminescence ($\sim 10^1$ counts) and thus a weak emission color. The emission of a core/shell QD is more intense ($\sim 10^6$ counts). It should be noted that the reported intensities in counts are concentration- and detector-dependent. The increase in intensity is due to the surface passivation of the InP core via inorganic ZnS shell formation. The shell layer is grown using a saturated solution of sulfur dissolved in trioctylphosphine (denoted as TOP-S) together with zinc stearate (dissolved in hexadecane⁵⁵), as shown in Scheme 2.

Even though the current experimental plan only allows for partial execution of the shelling procedure, the QDs show already a quite bright emission under UV light. Students recorded photoluminescence spectra of all the cores and core/

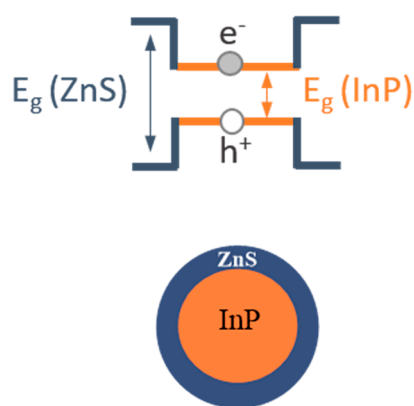


Figure 4. Schematic representation of the band alignment of InP/ZnS type-I heterojunction with the band gap (E_g) indicated for both materials. The electron and hole pair that is created upon photon absorption is depicted.

Scheme 2. Two-Step Synthetic Strategy to Obtain InP/ZnS Core/Shell Heterostructure QDs



shell structures and compared the relative intensities and wavelengths (Figure 5). A red shift of the emission is observed for increasing sizes. All emission spectra feature a rather large line width, which is likely due to broad size distributions.

Surface Chemistry by NMR Spectroscopy

The QD surface chemistry is studied using ^1H NMR spectroscopy.^{56,57} About 30 mg of the core QDs is dispersed in CDCl_3 . The resonances associated with ligands bound to the

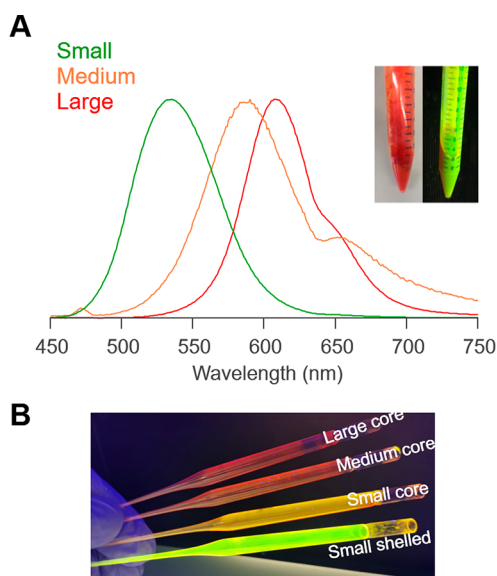


Figure 5. (A) Normalized photoluminescence spectra of the three core/shell synthesized QDs. The inset is a picture showing the difference in color of the small-sized core/shell QDs under normal light and UV light. (B) Picture showing the differences in color and intensity of the three different-sized cores and the small core/shell QDs under UV light.

QD surface appear broader than the resonances of, e.g., free oleylamine in CDCl_3 (Figure 6). Bound ligands feature both

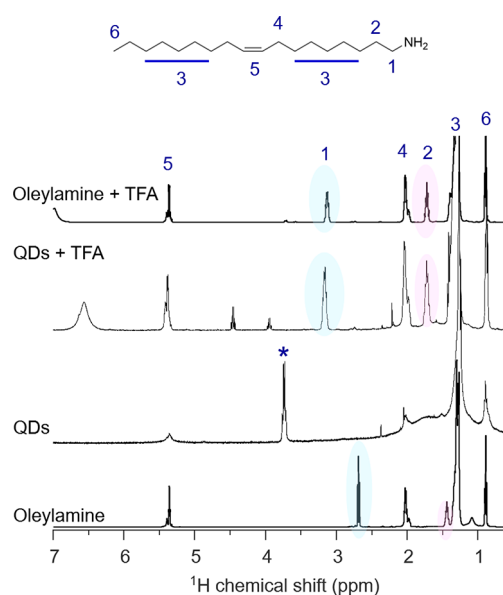


Figure 6. ^1H NMR spectra (400 MHz) of free oleylamine, purified QDs, QDs after TFA addition, and a reference of oleylamine with TFA. Resonances assigned to protonated oleylamine can be detected after the TFA addition due to ligand stripping. Resonances 1 and 2 (shaded regions) are shifted after TFA addition due to protonation of the amine. Ethanol (*) is also present in the initial solution as an impurity.

homogeneous and heterogeneous broadening.⁵⁶ The homogeneous line width is proportional to the T_2 relaxation rate and scales with the size of the object. Free oleylamine has a lot of rotational freedom and tumbles fast (slow T_2 relaxation), and it thus has sharp resonances. Oleylamine bound to a large QD has less rotational freedom, which results in faster relaxation and thus broader lines. Heterogeneous broadening results from the superposition of resonances that have different chemical environments and therefore slightly different chemical shifts. A well-solvated ligand shell has a quite uniform environment, while poorly solvated ligand shells feature many ligand–ligand interactions and thus more heterogeneous broadening. Both broadening mechanisms are size-dependent.⁵⁶

Given the broad resonances, it is difficult to unambiguously assign the identity of the ligand. Therefore, trifluoroacetic acid (TFA) is added to protonate the ligands, breaking the bond with the QD surface, and the QDs precipitate. In solution, the ligands have again sharp resonances and can be identified. After TFA addition, the students record a new ^1H NMR spectrum. This time the resonances of protonated oleylamine can be recognized at 3.2 and 1.7 ppm assigned to the α - and β - CH_2 of oleylammonium, respectively (Figure 6). The broad resonance around 6.5 ppm is assigned to a proton pool of exchangeable protons (H_2O and RNH_2).

The results are consistent with previous surface chemistry studies.^{42,58} Both chloride and oleylamine ligands are present at the QD surface (in the case of InCl_3 as the reagent) (see Figure 7). Chloride was detected with X-ray photoelectron spectroscopy, and such a measurement is outside the scope of this laboratory exercise. While oleylamine is a neutral Lewis base (L-type ligand), chloride is a negatively charged Lewis base (an X-type ligand). Given that the whole nanocrystal

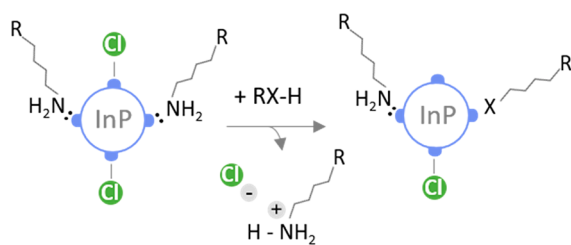


Figure 7. Schematic representation of the surface of the InP core obtained from InCl_3 .⁵⁸ Both oleylamine and chloride are present at the surface. Upon the addition of an acid, oleylammonium chloride is released from the surface and replaced by the conjugate base as an X-type (charged) ligand.

object must be charge-neutral in solvents with a low dielectric constant, the InP core must be indium-rich. The chloride-amine pair can be exchanged for other X-type ligands (e.g., carboxylic acids) with the removal of ammonium chloride as a byproduct (see Figure 7).⁵⁸

STUDENT LEARNING

Students prepare their lab notes based on literature and the handout. Together with an assistant, one team of two or three students prepares a 20 min presentation about every step of the synthesis and presents it to all students 1 week before the experiment. Afterward, every student must come with prepared lab notes including all calculations of the required precursor, a step-by-step description of the synthesis, and important hazards. The assistant checks the lab notes with each student individually and asks questions for 5–10 min. An unprepared student is not allowed to work in the lab. At the University of Basel, we believe that this method prepares the students to plan experiments based on research articles. In this article, we are providing all of the information so that other universities can choose how they want to proceed and how much information they want to provide to their students.

In these experiments, the students used air-free and hot-injection techniques to synthesize, isolate, and characterize colloidal stable nanocrystals. The students observed a trend in the optical properties with QD size. They then related the visual change in color to quantum confinement theory. Using UV-vis data, they determined the average size of their QDs as well as the yield of their reaction. Second, students became familiar with the concept of surface traps and how to passivate them with type-I heterostructures. They synthesized InP/ZnS core/shell QDs and visually observed an increase in brightness. Finally, the students investigated the surface chemistry by NMR spectroscopy, identifying the bound ligands. Students must succeed in the experiments in order to continue with the following ones. A report in a paper style is required within 2 weeks by each student, in which they must include relevant references in the introduction and present their data in a consistent way. The discussion part of these reports was our main method to assess whether the students understood the different concepts. If students had different results than the ones expected (e.g., lower yield or different size), they had to provide plausible reasoning for it and relate to how they conducted the experiment (longer reaction time, amount of precursor used). The example student report in the [Supporting Information](#) clearly indicates successful learning. We got positive feedback from the students that these experiments are enjoyable and exciting.

SCHEDULE

The students read the lab script and prepare their lab notes with the step-by-step procedure prior to the start of the lab section. Day 1 is a full day (8 hours). Each student team (one or two students) synthesizes three sizes of InP cores. The QDs are purified by both precipitation–redispersion and size exclusion chromatography methods. One InP core synthesis takes a maximum of 1.5 hours, including preparation, ramping, and heating time. Each student team performs one core synthesis in the morning and two syntheses in the afternoon. Since they are working as a team, the workload must be divided between the students, e.g., when one is setting up the next experiment, the other proceeds with the purification. Day 2 is an afternoon (5 hours). Each student team carries out one core/shell QD synthesis and its purification via precipitation redispersion. The assistants assign one size of core/shell QDs to each team, such that all sizes of core/shell QDs are synthesized within one lab. The core/shell QD synthesis takes about 4 hours, including at least 2 hours of waiting time. Characterizations (UV-vis and PL) of the previously synthesized cores are performed during the waiting times of the core/shell QD synthesis. Day 3 is another afternoon (5 h), which is used as a buffer day for students to finish up all of the syntheses and the UV-vis and PL characterizations of their products. This time can be easily split up over multiple shorter sessions. NMR experiments are performed on one of the core particles before and after ligand stripping with TFA. The students have 2 weeks to hand in a detailed protocol (in article style), with a discussion of their results.

HAZARDS

All personal protective equipment (PPE), including gloves, goggles, and lab coats, is worn at all times. Preparations are performed in a fume hood. If the students have no experience with Schlenk lines, we strongly advise them to read *The Schlenk Line Survival Guide* published by A. M. Borys.⁵⁹ Schlenk line use requires explicit training and supervision. Improper usage could lead to condensation of liquid oxygen in the cold trap, an explosion hazard. Tris(diethylamino)phosphine, TOP, and TOP-S are air-sensitive and reactive precursors that are stored under nitrogen. They are added to the reaction mixture with minimal contact with air. If the TOP bottle does not have a septum, either transfer the solution to a Schlenk flask or work under a constant nitrogen flow by using an upside-down funnel attached to the Schlenk line. Use a needle and syringe to add the precursors to the mixture. Make sure to flush the needle three times with nitrogen before taking the required volume. Bend the needle to suck up a protective layer of nitrogen in the syringe before adding the content to the three-neck flask via the septum. In the case of spillage, avoid the use of tissues—use sand instead. The evolution of diethylamine gas may have acute oral, inhalation, and skin toxicity with a 5 ppm TLV value, and handling flammable liquids at 180 °C may result in fire and burns. It is therefore very important to work under an inert atmosphere in a fume hood throughout the reaction. Trifluoroacetic acid is harmful if inhaled and causes severe skin burns and eye damage. While taking aliquots be aware that the solution is hot. Only take 100 μL of solution and proceed quickly with the ejection. An assistant must be present next to the student when the aliquot is taken. A beaker with isopropanol and/or sand must always be available next to

the student for any necessary quenching. Glass syringes are safer than plastic ones.

SUMMARY

We adapted the InP QDs synthesis for an undergraduate inorganic chemistry course so that students can enjoy making and characterizing QDs without being concerned with major toxicity issues of the chemicals used, such as cadmium or lead. InP/ZnS core/shell QDs of different colors were made with bright photoluminescence. Students were familiarized with concepts such as the quantum confinement effect, colloidal stability, and surface chemistry. The temperatures at which these reactions occur are rather low, and a sand bath can also be used instead of thermocontrollers. These syntheses are a robust and safe way for students to explore QDs for the first time.

ASSOCIATED CONTENT

Supporting Information

The Supporting Information is available at <https://pubs.acs.org/doi/10.1021/acs.jchemed.2c01167>.

- Experimental details (PDF)
- Student handout (PDF)
- Student report (PDF)
- XRD data file (TXT)

AUTHOR INFORMATION

Corresponding Author

Jonathan De Roo – Department of Chemistry, University of Basel, CH-4058 Basel, Switzerland; orcid.org/0000-0002-1264-9312; Email: Jonathan.DeRoo@unibas.ch

Authors

Mahsa Parvizia – Department of Chemistry, University of Basel, CH-4058 Basel, Switzerland

Julia Bechter – Department of Chemistry, University of Basel, CH-4058 Basel, Switzerland

Jan Huber – Department of Chemistry, University of Basel, CH-4058 Basel, Switzerland

Noura Chettata – Department of Chemistry, University of Basel, CH-4058 Basel, Switzerland

Complete contact information is available at: <https://pubs.acs.org/10.1021/acs.jchemed.2c01167>

Notes

The authors declare no competing financial interest.

ACKNOWLEDGMENTS

The authors thank Valentin Köhler for his support in the organization of the lab course and students Vera Jost, Joshua Böhler, and Anina Noemi Portmann for sharing their data and pictures. We thank the University of Basel for financial support.

REFERENCES

- (1) Matijevic, E. Preparation and Properties of Uniform Size Colloids. *Chem. Mater.* **1993**, *5* (4), 412–426.
- (2) Trindade, T.; O'Brien, P.; Pickett, N. L. Nanocrystalline Semiconductors: Synthesis, properties, and perspectives. *Chem. Mater.* **2001**, *13* (11), 3843–3858.
- (3) Kovalenko, M. V.; Manna, L.; Cabot, A.; Hens, Z.; Talapin, D. V.; Kagan, C. R.; Klimov, V. I.; Rogach, A. L.; Reiss, P.; Milliron, D. J.;

Guyot-Sionnest, P.; Konstantatos, G.; Parak, W. J.; Hyeon, T.; Korgel, B. A.; Murray, C. B.; Heiss, W. Prospects of Nanoscience with Nanocrystals. *ACS Nano* **2015**, *9* (2), 1012–1057.

(4) Baek, W.; Chang, H.; Bootharaju, M. S.; Kim, J. H.; Park, S.; Hyeon, T. Recent Advances and Prospects in Colloidal Nanomaterials. *JACS Au* **2021**, *1* (11), 1849–1859.

(5) Calvin, J. J.; Brewer, A. S.; Alivisatos, A. P. The role of Organic Ligand Shell Structures in Colloidal Nanocrystal Synthesis. *Nat. Synth.* **2022**, *1* (2), 127–137.

(6) Yin, Y.; Alivisatos, A. P. Colloidal Nanocrystal Synthesis and The Organic-Inorganic Interface. *Nature* **2005**, *437* (7059), 664–670.

(7) Park, J.; Joo, J.; Kwon, S. G.; Jang, Y.; Hyeon, T. Synthesis of Monodisperse Spherical Nanocrystals. *Angew. Chem., Int. Ed.* **2007**, *46* (25), 4630–4660.

(8) Xia, Y.; Xiong, Y.; Lim, B.; Skrabalak, S. E. Shape-Controlled Synthesis of Metal Nanocrystals: Simple Chemistry Meets Complex Physics? *Angew. Chem., Int. Ed.* **2009**, *48* (1), 60–103.

(9) Nasilowski, M.; Mahler, B.; Lhuillier, E.; Ithurria, S.; Dubertret, B. Two-Dimensional Colloidal Nanocrystals. *Chem. Rev.* **2016**, *116* (18), 10934–10982.

(10) Efros, A. L.; Brus, L. E. Nanocrystal Quantum Dots: From Discovery to Modern Development. *ACS Nano* **2021**, *15* (4), 6192–6210.

(11) Resch-Genger, U.; Grabolle, M.; Cavaliere-Jaricot, S.; Nitschke, R.; Nann, T. Quantum Dots Versus Organic Dyes as Fluorescent Labels. *Nat. Methods* **2008**, *5* (9), 763–775.

(12) Neeleshwar, S.; Chen, C. L.; Tsai, C. B.; Chen, Y. Y.; Chen, C. C.; Shyu, S. G.; Seehra, M. S. Size-Dependent Properties of CdSe Quantum Dots. *Phys. Rev. B* **2005**, *71* (20), 201307–201311.

(13) Murray, C. B.; Norris, D. J.; Bawendi, M. G. Synthesis and Characterization Of Nearly Monodisperse Cde (E = S, Se, Te) Semiconductor Nanocrystallites. *J. Am. Chem. Soc.* **1993**, *115* (19), 8706–8715.

(14) Van den Eynden, D.; Pokratath, R.; De Roo, J. Nonaqueous Chemistry of Group 4 Oxo Clusters and Colloidal Metal Oxide Nanocrystals. *Chem. Rev.* **2022**, *122* (11), 10538–10572.

(15) De Roo, J. Chemical Considerations for Colloidal Nanocrystal Synthesis. *Chem. Mater.* **2022**, *34* (13), 5766–5779.

(16) Mourdikoudis, S.; Liz-Marzan, L. M. Oleylamine in Nanoparticle Synthesis. *Chem. Mater.* **2013**, *25* (9), 1465–1476.

(17) Kister, T.; Monego, D.; Mulvaney, P.; Widmer-Cooper, A.; Kraus, T. Colloidal Stability of Apolar Nanoparticles: The Role of Particle Size and Ligand Shell Structure. *ACS Nano* **2018**, *12* (6), 5969–5977.

(18) Monego, D.; Kister, T.; Kirkwood, N.; Mulvaney, P.; Widmer-Cooper, A.; Kraus, T. Colloidal Stability of Apolar Nanoparticles: Role of Ligand Length. *Langmuir* **2018**, *34* (43), 12982–12989.

(19) Doblas, D.; Kister, T.; Cano-Bonilla, M.; González-García, L.; Kraus, T. Colloidal Solubility and Agglomeration of Apolar Nanoparticles in Different Solvents. *Nano Lett.* **2019**, *19* (8), 5246–5252.

(20) Kwon, S. G.; Hyeon, T. Colloidal Chemical Synthesis and Formation Kinetics of Uniformly Sized Nanocrystals of Metals, Oxides, and Chalcogenides. *Acc. Chem. Res.* **2008**, *41* (12), 1696–1709.

(21) Murray, C. B.; Kagan, C. R.; Bawendi, M. G. Synthesis and Characterization of Monodisperse Nanocrystals and Close-Packed Nanocrystal Assemblies. *Annu. Rev. Mater. Sci.* **2000**, *30* (1), 545–610.

(22) Park, J.; Joo, J.; Kwon, S. G.; Jang, Y.; Hyeon, T. Synthesis of Monodisperse Spherical Nanocrystals. *Angew. Chem., Int. Ed.* **2007**, *46* (25), 4630–4660.

(23) Abiodun, S. L.; Pellechia, P. J.; Greytak, A. B. Effective Purification of CsPbBr₃ Nanocrystals with High Quantum Yield and High Colloidal Stability via Gel Permeation Chromatography. *J. Phys. Chem. C* **2021**, *125* (6), 3463–3471.

(24) Shen, Y.; Gee, M. Y.; Tan, R.; Pellechia, P. J.; Greytak, A. B. Purification of Quantum Dots by Gel Permeation Chromatography and the Effect of Excess Ligands on Shell Growth and Ligand Exchange. *Chem. Mater.* **2013**, *25* (14), 2838–2848.

- (25) Shen, Y.; Gee, M. Y.; Greytak, A. B. Purification Technologies for Colloidal Nanocrystals. *Chem. Commun.* **2017**, 53 (5), 827–841.
- (26) Nordell, K. J.; Boatman, E. M.; Lisensky, G. C. A Safer, Easier, Faster Synthesis for CdSe Quantum Dot Nanocrystals. *J. Chem. Educ.* **2005**, 82 (11), 1697–1699.
- (27) Landry, M. L.; Morrell, T. E.; Karagounis, T. K.; Hsia, C.-H.; Wang, C.-Y. Simple Syntheses of CdSe Quantum Dots. *J. Chem. Educ.* **2014**, 91 (2), 274–279.
- (28) Shekhirev, M.; Goza, J.; Teeter, J. D.; Lipatov, A.; Sinitskii, A. Synthesis of Cesium Lead Halide Perovskite Quantum Dots. *J. Chem. Educ.* **2017**, 94 (8), 1150–1156.
- (29) Bauer, C. A.; Hamada, T. Y.; Kim, H.; Johnson, M. R.; Voegtle, M. J.; Emrick, M. S. An Integrated, Multipart Experiment: Synthesis, Characterization, and Application of CdS and CdSe Quantum Dots as Sensitizers in Solar Cells. *J. Chem. Educ.* **2018**, 95 (7), 1179–1186.
- (30) Yang, H.; Fan, W.; Hills-Kimball, K.; Chen, O.; Wang, L.-Q. Introducing Manganese-Doped Lead Halide Perovskite Quantum Dots: A Simple Synthesis Illustrating Optoelectronic Properties of Semiconductors. *J. Chem. Educ.* **2019**, 96 (10), 2300–2307.
- (31) Bennett, E.; Greenberg, M. W.; Jordan, A. J.; Hamachi, L. S.; Banerjee, S.; Billinge, S. J. L.; Owen, J. S. Size Dependent Optical Properties and Structure of ZnS Nanocrystals Prepared from a Library of Thioureas. *Chem. Mater.* **2022**, 34 (2), 706–717.
- (32) Toufanian, R.; Zhong, X.; Kays, J. C.; Saeboe, A. M.; Dennis, A. M. Correlating ZnSe Quantum Dot Absorption with Particle Size and Concentration. *Chem. Mater.* **2021**, 33 (18), 7527–7536.
- (33) Kuzuya, T.; Tai, Y.; Yamamuro, S.; Sumiyama, K. Size-Focusing of ZnS Nanocrystals Observed by MALDI-TOF Mass Spectroscopy. *Chem. Phys. Lett.* **2005**, 407 (4), 460–463.
- (34) Li, L. S.; Pradhan, N.; Wang, Y.; Peng, X. High Quality ZnSe and ZnS Nanocrystals Formed by Activating Zinc Carboxylate Precursors. *Nano Lett.* **2004**, 4 (11), 2261–2264.
- (35) Lisensky, G.; McFarland-Porter, R.; Paquin, W.; Liu, K. Synthesis and Analysis of Zinc Copper Indium Sulfide Quantum Dot Nanoparticles. *J. Chem. Educ.* **2020**, 97 (3), 806–812.
- (36) Won, Y. H.; Cho, O.; Kim, T.; Chung, D. Y.; Kim, T.; Chung, H.; Jang, H.; Lee, J.; Kim, D.; Jang, E. Highly Efficient and Stable InP/ZnSe/ZnS Quantum Dot Light-Emitting Diodes. *Nature* **2019**, 575 (7784), 634–638.
- (37) Reiss, P.; Carriere, M.; Lincheneau, C.; Vaure, L.; Tamang, S. Synthesis of Semiconductor Nanocrystals, Focusing on Nontoxic and Earth-Abundant Materials. *Chem. Rev.* **2016**, 116 (18), 10731–10819.
- (38) Tessier, M. D.; Dupont, D.; De Nolf, K.; De Roo, J.; Hens, Z. Economic and Size-Tunable Synthesis of InP/ZnE (E = S, Se) Colloidal Quantum Dots. *Chem. Mater.* **2015**, 27 (13), 4893–4898.
- (39) Tessier, M. D.; De Nolf, K.; Dupont, D.; Sinnaeve, D.; De Roo, J.; Hens, Z. Aminophosphines: A Double Role in the Synthesis of Colloidal Indium Phosphide Quantum Dots. *J. Am. Chem. Soc.* **2016**, 138 (18), 5923–5929.
- (40) Buffard, A.; Dreyfuss, S.; Nadal, B.; Heuclin, H.; Xu, X.; Patriarche, G.; Mézailles, N.; Dubertret, B. Mechanistic Insight and Optimization of InP Nanocrystals Synthesized with Aminophosphines. *Chem. Mater.* **2016**, 28 (16), 5925–5934.
- (41) McMurtry, B. M.; Qian, K.; Teglas, J. K.; Swarnakar, A. K.; De Roo, J.; Owen, J. S. Continuous Nucleation and Size Dependent Growth Kinetics of Indium Phosphide Nanocrystals. *Chem. Mater.* **2020**, 32 (10), 4358–4368.
- (42) Kim, K.; Yoo, D.; Choi, H.; Tamang, S.; Ko, J. H.; Kim, S.; Kim, Y. H.; Jeong, S. Halide-Amine Co-Passivated Indium Phosphide Colloidal Quantum Dots in Tetrahedral Shape. *Angew. Chem., Int. Ed.* **2016**, 55 (11), 3714–3718.
- (43) Evans, J. S. O.; Evans, I. R. Structure Analysis from Powder Diffraction Data: Rietveld Refinement in Excel. *J. Chem. Educ.* **2021**, 98 (2), 495–505.
- (44) Holder, C. F.; Schaak, R. E. Tutorial on Powder X-ray Diffraction for Characterizing Nanoscale Materials. *ACS Nano* **2019**, 13 (7), 7359–7365.
- (45) Chon, J. W. M.; Gu, M.; Bullen, C.; Mulvaney, P. Three-Photon Excited Band Edge and Trap Emission of CdS Semiconductor Nanocrystals. *Appl. Phys. Lett.* **2004**, 84 (22), 4472–4474.
- (46) Hens, Z.; Moreels, I. Light Absorption by Colloidal Semiconductor Quantum Dots. *J. Mater. Chem.* **2012**, 22 (21), 10406–10415.
- (47) Anderson, N. C.; Hendricks, M. P.; Choi, J. J.; Owen, J. S. Ligand Exchange and the Stoichiometry of Metal Chalcogenide Nanocrystals: Spectroscopic Observation of Facile Metal-Carboxylate Displacement and Binding. *J. Am. Chem. Soc.* **2013**, 135 (49), 18536–18548.
- (48) Kirkwood, N.; Monchen, J. O. V.; Crisp, R. W.; Grimaldi, G.; Bergstein, H. A.; du Fossé, I.; van der Stam, W.; Infante, I.; Houtepen, A. J. Finding and Fixing Traps in II-VI and III-V Colloidal Quantum Dots: The Importance of Z-type Ligand Passivation. *J. Am. Chem. Soc.* **2018**, 140 (46), 15712–15723.
- (49) Houtepen, A. J.; Hens, Z.; Owen, J. S.; Infante, I. On the Origin of Surface Traps in Colloidal II-VI Semiconductor Nanocrystals. *Chem. Mater.* **2017**, 29 (2), 752–761.
- (50) Jang, Y.; Shapiro, A.; Isarov, M.; Rubin-Brusilovski, A.; Safran, A.; Budniak, A. K.; Horani, F.; Dehnel, J.; Sashchiuk, A.; Lifshitz, E. Interface Control Of Electronic And Optical Properties in IV-VI and II-VI Core/Shell Colloidal Quantum Dots: A Review. *Chem. Commun.* **2017**, 53 (6), 1002–1024.
- (51) Giansante, C.; Infante, I. Surface Traps in Colloidal Quantum Dots: A Combined Experimental and Theoretical Perspective. *J. Phys. Chem. Lett.* **2017**, 8 (20), 5209–5215.
- (52) Dabbousi, B. O.; Rodriguez-Viejo, J.; Mikulec, F. V.; Heine, J. R.; Mattoussi, H.; Ober, R.; Jensen, K. F.; Bawendi, M. G. (CdSe)ZnS Core-Shell Quantum Dots: Synthesis and Characterization of a Size Series of Highly Luminescent Nanocrystallites. *J. Phys. Chem. B* **1997**, 101 (46), 9463–9475.
- (53) Xie, R.; Kolb, U.; Li, J.; Basche, T.; Mews, A. Synthesis and Characterization of Highly Luminescent CdSe-Core CdS/ZnO.SCd0.5S/ZnS Multishell Nanocrystals. *J. Am. Chem. Soc.* **2005**, 127 (20), 7480–7488.
- (54) Mahler, B.; Spinicelli, P.; Buil, S.; Quelin, X.; Hermier, J. P.; Dubertret, B. Towards Non-Blinking Colloidal Quantum Dots. *Nat. Mater.* **2008**, 7 (8), 659–664.
- (55) Dhaene, E.; Billet, J.; Bennett, E.; Van Driessche, I.; De Roo, J. The Trouble with ODE: Polymerization during Nanocrystal Synthesis. *Nano Lett.* **2019**, 19 (10), 7411–7417.
- (56) De Roo, J.; Yazdani, N.; Drijvers, E.; Lauria, A.; Maes, J.; Owen, J. S.; Van Driessche, I.; Niederberger, M.; Wood, V.; Martins, J. C.; Infante, I.; Hens, Z. Probing Solvent-Ligand Interactions in Colloidal Nanocrystals by the NMR Line Broadening. *Chem. Mater.* **2018**, 30 (15), 5485–5492.
- (57) Hens, Z.; Martins, J. C. A Solution NMR Toolbox for Characterizing the Surface Chemistry of Colloidal Nanocrystals. *Chem. Mater.* **2013**, 25 (8), 1211–1221.
- (58) Leemans, J.; Dumbgen, K. C.; Minjauw, M. M.; Zhao, Q.; Vantomme, A.; Infante, I.; Detavernier, C.; Hens, Z. Acid-Base Mediated Ligand Exchange on Near-Infrared Absorbing, Indium-Based III-V Colloidal Quantum Dots. *J. Am. Chem. Soc.* **2021**, 143 (11), 4290–4301.
- (59) Borys, A. M. *The Schlenk Line Survival Guide*. <https://schlenklinesurvivalguide.com>.